Eur. Phys. J. Special Topics **208**, 67–74 (2012)

DOI: 10.1140/epjst/e2012-01607-2

THE EUROPEAN PHYSICAL JOURNAL SPECIAL TOPICS

Regular Article

Determination of absolute chirality using resonant X-ray diffraction

Y. Tanaka[1,a] and S.W. Lovesey[2]

[1] RIKEN SPring-8 Centre, Sayo, Hyogo 679-5148, Japan
[2] ISIS Facility and Diamond Light Source Ltd., Didcot, Oxfordshire OX11 0QX, UK

Received 8 December 2011 / Received in final form 23 March 2012
Published online 15 June 2012

Abstract. We have demonstrated that resonant diffraction experiments using the circularly polarized X-ray beam *absolutely* determines the crystal chirality. Both berlinite and quartz crystals belonging to space group $P3_221$ show higher azimuth-constant intensity for the negative $(-)$ helicity beam than that for the the positive $(+)$ helicity beam for space-group forbidden reflection 001. The relation is opposite for quartz crystal belonging to space group $P3_121$. Theoretical calculation shows that this relation completely agrees with the experimental findings for the enantiomorphic space-group pair $P3_121$ and $P3_221$. This method is applicable to chiral motifs that occur in biomolecules, liquid crystals, ferroelectrics, and multiferroics, etc.

1 Introduction

The concept of chirality often plays a quite important role in physics, chemistry and biology. For example, the occurrence of homochirality in amino acids and sugars is an essential enigma in biology, possibly related to the formation of life.

Low quartz (SiO_2), berlinite ($AlPO_4$) and tellurium have an enantiomer pair, $P3_121$ (#152, right-handed screw) and $P3_221$ (#154, left-handed screw). X-ray diffraction with dispersion correction terms has been playing an important role in determining the handedness of enantiomers for a long time. Experiments can be done conveniently in the laboratory by choosing a proper (rotating) anode. We have developed a completely different method to determine the crystal handedness using resonant diffraction with circularly polarized X-rays. Our results demonstrate that positive and negative circularly polarized X-rays at the resonant energy of low quartz (Si 1s edge) [1–3], berlinite (Al 1s edge) [4,5], and tellurium (Te 2s edge) [6] identify the absolute structure (right or left-handed). In the present paper, we discuss the method of determining the absolute chirality using resonant X-ray diffraction. Our method is applicable to a subset of non-symmorphic space groups that possess an enantiomorphic screw-axis, 3_1, 4_1, 6_1, 6_2 for right-handed, and 3_2, 4_3, 6_5, 6_4 for left-handed, in addition to the magnetic chirality with a helical screw structure [7].

[a] e-mail: ytanaka@riken.jp

Table 1. The phase of the electric field, the scattering vector, the sign of f'' and the structure factor.

	Phase of electric field	Scattering vector	Sign of f''	Structure factor
Quantum mechanics [11]	$\mathbf{E}\exp i(\mathbf{k}\cdot\mathbf{r}-\omega t)$	$\mathbf{K}=\mathbf{k}_i-\mathbf{k}_f$	$-$	$F=\sum_j f_j \exp i(\mathbf{K}\cdot\mathbf{r})$
Crystallographer [14]	$\mathbf{E}\exp i(\omega t-\mathbf{k}\cdot\mathbf{r})$	$\mathbf{K}=\mathbf{k}_f-\mathbf{k}_i$	$+$	$F=\sum_j f_j \exp i(\mathbf{K}\cdot\mathbf{r})$
Others	$\mathbf{E}\exp i(\mathbf{k}\cdot\mathbf{r}-\omega t)$	$\mathbf{K}=\mathbf{k}_f-\mathbf{k}_i$	$-$	$F=\sum_j f_j \exp i(-\mathbf{K}\cdot\mathbf{r})$

The essential concept of our method is coupling of a chiral structure with a chiral probe. The desired coupling is absent if the structure is achiral, including structures that contain a neutral screw-axis like 2_1.

Determining the absolute chirality is quite a delicate matter [8]. One mistake or an odd number of mistakes leads us to the opposite answer. However once the relation between the structure and some external macroscopic physical property like the optical rotatory power is established, there is no need to measure the structure for each crystal. The X-ray diffraction has a long history since the discovery of Bragg's law, however, there is no consensus in the literature on the definition of variables in the unit-cell structure factor. Historically crystallographers have used to the expression $\exp i(\omega t - kz)$ for an electromagnetic plane wave which propagates along the positive z direction with the propagation vector $\mathbf{k} = k\hat{\mathbf{z}}$. Here the wave number $k > 0$, the wave frequency $\omega > 0$ and $\hat{\mathbf{z}}$ is the unit vector along the z axis. On the other hand, the same electromagnetic wave is expressed by $\exp i(kz - \omega t)$ in quantum mechanics. These conventions are not usually written explicitly in the literature. Fortunately misinterpretation rarely happens because most papers for the crystallography implicitly use the former one and moreover two conventions do not make any difference in the analysis as far as the symmetric crystalline or magnetic structures are concerned. However once the polarity or the handedness of crystals is a matter of discussion, we need to understand the difference correctly. Non-trivial problems can arise when the two conventions are mixed. The atomic scattering length is $f = f_0 + f' + if''$ where f' and f'' are the dispersion correction terms. The sign of f'', for example, depends on which convention is used. Table 1 shows a summary of the phase factor of the electric field, the sign of the scattering vector, the sign of f'' and the structure factor.

2 Atomic structure

Low-quartz (SiO_2) and berlinite ($AlPO_4$) have enantiomers belonging to a space-group pair, #152 (right-handed screw) and #154 (left-handed screw). These space groups are mirror images of each other. Berlinite ($AlPO_4$) has the similar atomic structure to quartz, obtained by replacing Si with Al and P atoms alternatively along the c axis. Hereafter we use the terms R quartz and R berlinite for the crystal structure which belongs to the space group #152 and L quartz and L berlinite for the crystal structure which belongs to the space group #154. The atomic configurations of R quartz and L berlinite are shown in Fig. 1. The alternative replacement of Si atoms of quartz with Al and P atoms changes the sign of chirality together with the space group, and doubles the lattice constant along the c axis, but does not change the position of oxygen atoms.

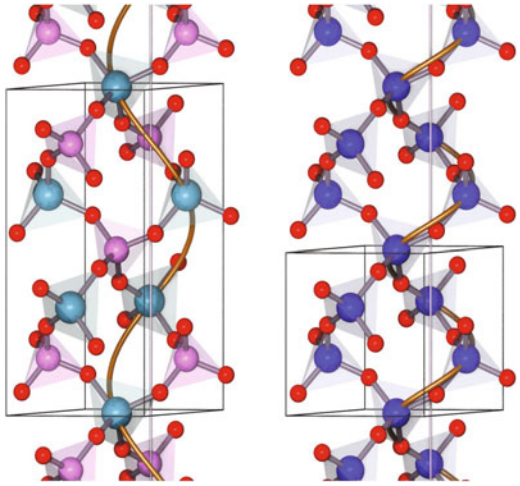

Fig. 1. (Adopted from Ref. [4,5]) Atomic structures of R quartz (right panel) and L berlinite (left panel). Blue and red spheres represent Si and O atoms, respectively in quartz, and light blue, pink, and red spheres represent Al, P, and O atoms, respectively in berlinite. A white line in each panel is one of the 3-fold screw axes and a screw line is a guide to eyes. Black lines show the unit cell for each crystal.

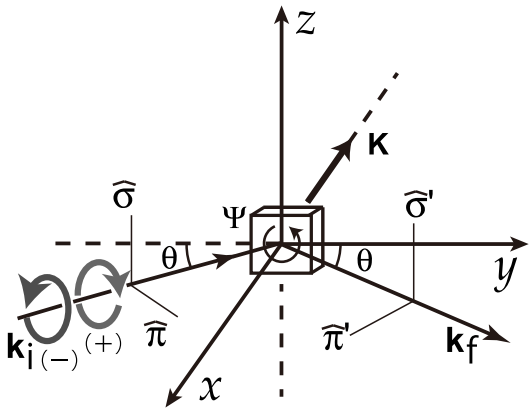

Fig. 2. A schematic view for Bragg diffraction with a right-handed coordinates x, y, and z. The scattering vector $\mathbf{K} = \mathbf{k}_i - \mathbf{k}_f$ is antiparallel to the x axis. The marks $(+)$ and $(-)$ denote the helicity of the incident beam (See the text). Here $\mathbf{k}_i$ and $\mathbf{k}_f$ are the propagation vectors of the incident and diffracted x rays, respectively, and θ denotes the Bragg angle. The $\hat{\sigma}$ and $\hat{\sigma}'$ components are perpendicular to the plane of scattering, and the $\hat{\pi}$ and $\hat{\pi}'$ components are parallel to the plane of scattering, $\hat{\pi} = (\cos\theta, \sin\theta, 0)$ and $\hat{\pi}' = (\cos\theta, -\sin\theta, 0)$.

3 Resonant X-ray diffraction

3.1 Circular polarization

The general diffraction geometry is illustrated in Fig. 2. The plane of scattering is spanned by two vectors $\mathbf{k}_i$ and $\mathbf{k}_f$, which are the propagation vectors of the incident and diffracted beams, respectively. The vectors for the incident (diffracted) beam $\hat{\sigma}$ ($\hat{\sigma}'$) and $\hat{\pi}$ ($\hat{\pi}'$) are chosen to be perpendicular and parallel, respectively, to the plane of scattering. Vectors $\mathbf{k}_i$, $\hat{\sigma}$, and $\hat{\pi}$ have the right-handed relation $\frac{\mathbf{k}_i}{|\mathbf{k}_i|} = \hat{\sigma} \times \hat{\pi}$,

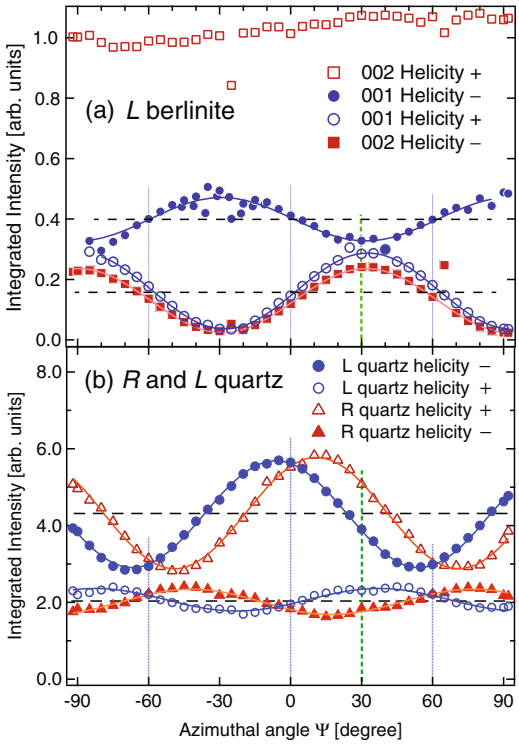

Fig. 3. (a) Integrated intensity of reflection 001 and 002 as a function of azimuthal angle for L berlinite. Filled circles (squares) represent the intensity of reflection 001 (002) measured with the incident beam with $(-)$ helicity and open circles (squares) represent the intensity of reflection 001 (002) measured with $(+)$ helicity. (Modified from Ref. [4,5]) (b) Integrated intensity of reflection 001 for R quartz and L quartz as a function of azimuthal angle. Filled and open circles (triangles) represent the intensity of reflection 001 of L quartz (R quartz) measured with the incident beam with $(-)$ helicity and $(+)$ helicity, respectively. (Modified from Ref. [1,2].) Each line shows a result of fit to data with functions expressed by Eq. (1) for panel (a) and Eq. (2) for panel (b).

and similarly for $\mathbf{k}_f$, $\hat{\sigma}'$ and $\hat{\pi}'$. The polarization state of the X-ray beam is generally expressed by the Stokes parameters P_1, P_2 and P_3 [9, 10]. Here $P_3 = +1, -1$ represent linear polarization along the vectors $\hat{\sigma}$ and $\hat{\pi}$, respectively, and $P_1 = +1, -1$ represent linear polarization along the vectors $\frac{1}{\sqrt{2}}(\hat{\sigma}+\hat{\pi})$ and $\frac{1}{\sqrt{2}}(\hat{\sigma}-\hat{\pi})$, respectively. Moreover $P_2 = +1, -1$ represent circular polarization (helicity). For positive $(+)$ helicity one has $\hat{\pi} = +i\hat{\sigma}$, and $\hat{\pi}$ lags $\hat{\sigma}$ by 90° according to the time phase-factor derived from $\exp i(kz - \omega t)$, and $\hat{\pi} = -i\hat{\sigma}$ for negative $(-)$ helicity. In other words, the $(+)$ and $(-)$ helicity beam has the counter-clockwise and clockwise motion, respectively, of the electric field, when an observer on the beam looks at the beam source as shown in Fig. 2. The azimuthal angle Ψ is a rotation of the sample about the scattering vector $\mathbf{K} = \mathbf{k}_i - \mathbf{k}_f$. The positive direction of Ψ is counter-clockwise as viewed looking up along the scattering vector $\mathbf{K}$.

3.2 Azimuthal-angle scans

Experiments were performed the beamline 17SU at SPring-8 in Harima, Japan [13]. The helicity of the incident beam was switched by the electromagnet of the undulator [14]. Figure 3 shows the azimuth scans of forbidden reflections 001 and 002 for L

Table 2. Inferred values of I_0, I_1, I_2 obtained by a fit to the experimental data with Eq. (1) for L berlinite and Eq. (2) for R and L quartz. Spaces with a dash denote null values, to a good approximation.

	Reflection	P_2	P_3	I_0	I_1	νI_2
L berlinite	001	+0.95	+0.30	0.162	0.125	—
L berlinite	001	−0.95	+0.30	0.399	−0.071	—
L berlinite	002	+0.95	+0.30	1.03	—	—
L berlinite	002	−0.95	+0.30	0.130	0.105	—
L quartz	001	+0.95	−0.31	2.06	+0.27	−0.11
L quartz	001	−0.95	−0.31	4.29	−0.44	+1.32
R quartz	001	+0.95	−0.31	4.32	−0.77	+1.21
R quartz	001	−0.95	−0.31	2.01	+0.26	−0.20

berlinite and forbidden reflection 001 for R quartz and L quartz. The handedness (chirality) of these samples were determined by the direction of the optical rotatory power beforehand. They were observed at Al $1s$ absorption edge ($E = 1567\,\mathrm{eV}$) and at Si $1s$ absorption edge ($E = 1848\,\mathrm{eV}$), respectively. The Stokes parameters are given by the insertion device parameters. At $E = 1567\,\mathrm{eV}$, they are $(P_1, P_2, P_3) = (0, \pm 0.95, +0.30)$ for the positive $(+)$ and negative $(-)$ helicity of the circularly polarized incident beam, respectively. At $E = 1848\,\mathrm{eV}$, they are $(P_1, P_2, P_3) = (0, \pm 0.95, -0.31)$ for the circularly polarized incident beam. The value of P_3 (degree of linear polarization) is unchanged by switching the helicity of the incident beam. The origin of the azimuth angle Ψ is defined with respect to the direction of the reciprocal lattice vector a^* axis when it is parallel to the z axis for L berlinite and L quartz and antiparallel to the z-axis for R quartz. The signs of helicity of the incident beam assigned in the previous papers [1,2,4,5] are in error and reversed here.

The scan curves of the integrated intensity I for L berlinite, except reflection 002 for $(+)$ helicity, and R and L quartz are nicely fitted to functions

$$I = I_0(P_2) + I_1(P_2)\cos\{3(\Psi - 30)\} \tag{1}$$

and

$$I = I_0(P_2) + I_1(P_2)\cos\{3(\Psi \mp 30)\} + \nu I_2(P_2)\sin\{3(\Psi \mp 30)\}, \tag{2}$$

respectively. Here the upper and lower signs are for L quartz and R quartz, respectively. This is required because the origin of the azimuth angle Ψ was defined to be upside-down for R quartz. The inferred values of the parametes are listed in Table 2. We find that $I_0(+) < I_0(-)$ for L berlinite reflection 001 and $I_0(+) > I_0(-)$ for L berlinite reflection 002 and that $I_0(+) < I_0(-)$ for L quartz reflection 001 while $I_0(+) > I_0(-)$ for R quartz reflection 001. Here we use $I_0(\pm) = I_0(P_2 = \pm 0.95)$ for simplicity. In the following discussion we show how azimuth-constant term I_0 works to determine the *absolute chirality* in the resonant diffraction using the circularly polarized X-rays. The asymmetric intensity I_2 of the azimuth scans observed in R quartz and L quartz originates from the $E1E2$ resonant event.

4 Discussion and summary

The intensity I of the resonant diffraction is described using the Stokes parameters $(P_1 = 0,\ P_2,\ P_3)$, $P_2 =$ helicity, as

$$\begin{aligned} I = {} & \tfrac{1}{2}(1 + P_3)\left(|G_{\sigma'\sigma}|^2 + |G_{\pi'\sigma}|^2\right) + \tfrac{1}{2}(1 - P_3)\left(|G_{\pi'\pi}|^2 + |G_{\sigma'\pi}|^2\right) \\ & + P_2 \mathrm{Im}\left(G^*_{\sigma'\pi}G_{\sigma'\sigma} + G^*_{\pi'\pi}G_{\pi'\sigma}\right). \end{aligned} \tag{3}$$

Here the quantum-mechanics expression $\exp i(kz - \omega t)$ is applied. This equation is readily derived either following the discussion of polarization in Ref. [10], or immediately from Eqs. (24) and (26) in Ref. [15]. Here $G_{\mu'\nu} = \sum d(E) F_{\mu'\nu}$ is the total resonant scattering amplitude, and μ' and ν are the polarization state of the diffracted and incident X-ray beam, respectively, $F_{\mu'\nu}$ is the scattering amplitude for a single resonant event and $d(E)$ is the energy profile for each event. The third term represents the interference between σ and π components in the resonant scattering and plays a crucial role to determine the absolute chirality by changing the sign coupling with the helicity. This σ-π interference term does not appear when $P_2 = 0$ and does not appear in conventional diffraction (Thomson scattering) even when $P_2 \neq 0$ because there are no events which change the polarization state ($\sigma \to \pi'$ or $\pi \to \sigma'$). In the following discussion we see that the interference term for the space groups #152 and #154 has a definite sign and that the sign is opposite to each other.

The structure factor for the enantiomorphic space-group pair $P3_121$ (#152) and $P3_221$ (#154) is fully described in Ref. [3]. For the space groups #152 and #154, Al (Si) atoms locate at $(-x,\ -x,\ 0)$, $(x,\ 0,\ \pm\frac{1}{3})$, and $(x,\ 0,\ \mp\frac{1}{3})$ in a unit cell of berlinite (quartz). Here the upper and lower sign of $\frac{1}{3}$ represent the space groups #152 and #154, respectively. The c axis is pointing along the $-x$ axis in Fig. 2. The most probable resonant process at the main peak of the absorption edges of Al and Si is the $E1E1$ event. The atomic multipole related to the $E1E1$ event is $\langle T_Q^K \rangle$. Here rank K and its projection Q satisfy $K = 2$ and $-K \leq Q \leq K$, with $\langle T_Q^K \rangle^* = (-1)^Q \langle T_{-Q}^K \rangle$ and the real $\langle T_Q^K \rangle'$ and imaginary $\langle T_Q^K \rangle''$ components defined such that $\langle T_Q^K \rangle = \langle T_Q^K \rangle' + i \langle T_Q^K \rangle''$. The unit-cell structure factor for #152 and #154, and reflection $00l$ ($l > 0$) is found to be

$$\Psi_Q^{(2)} = \langle T_Q^2 \rangle \left\{ 1 + \mathrm{e}^{2\pi i Q/3} \mathrm{e}^{2\pi i(\pm l/3)} + \mathrm{e}^{-2\pi i Q/3} \mathrm{e}^{2\pi i(\mp l/3)} \right\}. \tag{4}$$

Here we find the selection rule for reflection $00l$ that $l + Q = 3n$ for space group #152 and $l - Q = 3n$ for space group #154, where n is an integer. The four amplitudes for space-group forbidden reflections for the parity-even event $E1E1$ event together with parity odd event $E1E2$ or $E1M1$ are

$$G_{\sigma'\sigma} = T_a + \nu U_a \mathrm{e}^{i\eta}, \tag{5}$$

$$G_{\pi'\pi} = T_a \sin^2\theta + \nu U_b \mathrm{e}^{i\eta}, \tag{6}$$

$$G_{\pi'\sigma} = i \left\{ \nu T_a \sin\theta + U_\alpha \mathrm{e}^{i\eta} + \left(\nu T_\beta + U_\beta \mathrm{e}^{i\eta} \right) \mathrm{e}^{-3i\nu\Psi} \right\}, \tag{7}$$

$$G_{\sigma'\pi} = i \left\{ -\nu T_a \sin\theta - U_\alpha \mathrm{e}^{i\eta} + \left(\nu T_\beta + U_\beta \mathrm{e}^{i\eta} \right) \mathrm{e}^{-3i\nu\Psi} \right\}. \tag{8}$$

A parameter $\nu = \pm 1$ is introduced to label the chirality. For forbidden reflection 001, $\nu = +1$ represents space group #152 and $\nu = -1$ represents #154, respectively, but the sign reverses for forbidden reflection 002. Here θ denotes the Bragg angle. We use purely real quantities $T_a = \frac{3}{2} \langle T_{+2}^2 \rangle'$ and $T_\beta = \frac{3}{2} \langle T_{+1}^2 \rangle'' \cos\theta$ for quadrupoles and U_f ($f = a, b, \alpha$ and β) for parity-odd multipoles that are read off from the appendices in Ref. [3]. We obtain the intensity I only for a single $E1E1$ event, ignoring U_f terms,

$$I = I_0 + I_1 \cos 3\Psi, \tag{9}$$

$$I_0 = \tfrac{1}{2} \left\{ T_a^2 \left(1 + \sin^2\theta \right)^2 + 2T_\beta^2 \right\} + \tfrac{1}{2} P_3 T_a^2 \left(1 + \sin\theta \right)^2 \cos^2\theta, \\ + P_2 \nu T_a^2 \sin\theta \left(1 + \sin^2\theta \right), \tag{10}$$

$$I_1 = 2P_3 T_a T_\beta \sin\theta - P_2 \nu \cos\theta T_a T_\beta, \tag{11}$$

and the intensity I including the interference between an $E1E1$ event and $E1E2$ or $E1M1$ events,

$$I = I_0 + I_1 \cos 3\Psi + I_2 \sin 3\nu\Psi \tag{12}$$

$$\begin{aligned} I_0 = \tfrac{1}{2}\Big\{ & T_a^2\left(1+\sin^2\theta\right)^2 + U_a^2 + U_b^2 + 2U_\alpha^2 + 2\left(T_\beta^2 + U_\beta^2\right) \\ & + 2\nu\cos\eta\left[T_a\left(U_a + U_b\sin^2\theta\right) + 2\left(T_a U_\alpha \sin\theta + T_\beta U_\beta\right)\right] \\ & + P_3\left[T_a^2\cos^2\theta\left(1+\sin^2\theta\right) + U_a^2 - U_b^2 + 2\nu\cos\eta T_a(U_a - U_b\sin^2\theta)\right]\Big\} \\ & + P_2\left[\nu\left\{T_a^2\sin\theta\left(1+\sin^2\theta\right) + U_\alpha\left(U_a+U_b\right)\right\}\right. \\ & \left. + \cos\eta\left\{T_a\left(U_a+U_b\right)\sin\theta + T_a U_\alpha(1+\sin^2\theta)\right\}\right], \end{aligned} \tag{13}$$

$$\begin{aligned} I_1 = {} & 2P_3\left[T_a T_\beta \sin\theta + U_\alpha U_\beta + \nu\cos\eta\left\{T_a U_\beta\sin\theta + T_\beta U_\alpha\right\}\right] \\ & + P_2\left[\nu\left\{U_\beta\left(U_b - U_a\right) - T_a T_\beta\cos^2\theta\right\}\right. \\ & \left. + \cos\eta\left\{T_\beta\left(U_b - U_a\right) - T_a U_\beta\cos^2\theta\right\}\right], \end{aligned} \tag{14}$$

$$I_2 = -\sin\eta\left\{2P_3\left(T_\beta U_\alpha - T_a U_\beta\sin\theta\right) + \nu P_2\left(T_a U_\beta\cos^2\theta + T_\beta\left(U_b - U_a\right)\right)\right\}. \tag{15}$$

Here $E1E1$ and $E1E2$ or $E1M1$ events, each of which is not necessarily a single event, but assuming to be a single event for simplicity, are connected by the mixing parameter as $d_o(E)/d_e(E) = \exp(i\eta)\,|d_o(E)/d_e(E)|$, and $d_e(E)$ and $d_o(E)$ are the energy profile for the $E1E1$ and $E1E2$ or $E1M1$ events, respectively. In both cases, the azimuth-constant and σ-π interference term $I_{0,\mathrm{int}} = P_2\nu T_a^2\sin\theta(1+\sin^2\theta)$ found in Eq. (10) determines the absolute chirality by its sign. Because T_a is purely real and $T_a^2 \geq 0$, the intensity $I_{0,\mathrm{int}}$ has a definite sign corresponding to the helicity of the beam, P_2, as well as the crystal chirality, ν as long as $T_a \neq 0$.

Let us discuss the experimental results with above equations. The experimental data for L berlinite is simply expressed by Eq. (9) corresponding to the fitting function (1). As seen in Table 2 there is no I_2 contribution which is a product of the interference between the parity-even and the parity-odd events. Here we find that *the absolute sign* of $I_{0,\mathrm{int}}$ completely agrees with the experimental results: $I_0(+) < I_0(-)$ for L berlinite reflection 001 ($\nu = -1$) and $I_0(+) > I_0(-)$ for L berlinite reflection 002 ($\nu = +1$). The same argument is applicable to the tellurium results [6]. At the main resonant energies of Al $1s$ for berlinite and of Te $2s$ for tellurium, we found that the contribution of the parity-odd resonant events is negligible. Similarly we find that $I_0(+) < I_0(-)$ for L quartz reflection 001 ($\nu = -1$) while $I_0(+) > I_0(-)$ for R quartz reflection 001 ($\nu = +1$) in Table 2. Consequently, we find that *the absolute sign* of $I_{0,\mathrm{int}}$ completely agrees with the experimental results and that the observed chirality of the samples matches to the chirality determined by the optical activity as well as L berlinite. Thus we conclude that *the azimuth-constant intensity I_0 depends on the helicity of the circular polarization as well as the crystal chirality and that it determines the absolute chirality.* However, in case of quartz, the experimental data should be expressed by Eq. (12) corresponding to the fitting function (2) because of the non-negligible additional I_2 contribution as shown in Table 2.

In principle, both of the space-groups #152 and #154 have no inversion symmetry and can associate the parity-odd resonant event, deriving from the parity-odd multipoles due to the strong covalent bonding between oxygen atoms with silicon ions in quartz, or with aluminum ions in berlinite. The covalence effect might be much weaker in berlinite than in quartz. N. Thong and D. Schwarzenbach have suggested that the Al-O bond is less covalent compared to the P-O bond [16]. Let us discuss more about Eqs. (12) to (15). As we see, a one-to-one correspondence between the chirality (ν) and photon helicity (P_2) is kept only in I_2 but is lost in I_0 and I_1 that contains contributions $\nu\cos\eta$ and $P_2\cos\eta$. Therefore when the parity-even and parity-odd events

have an interference, it is inferred that strict determination of the chirality might be difficult because of many unknown parameters. The one-to-one correspondence in I_0 and I_1 is achieved when $\cos\eta = 0$ or, alternatively, the coefficients of $\nu\cos\eta$ and $P_2\cos\eta$ vanish. The latter condition occurs only for a single resonant event, because all coefficients of $\cos\eta$ are products of parity-even multipoles T and parity-odd multipoles U that vanish if one event is eliminated, $T = 0$ or $U = 0$. Note that the parity-even(-odd) resonant event observes only the parity-even(-odd) multipoles but not the parity-odd(-even) multipoles. The alternative condition $\cos\eta = 0$ is satisfied when the $E1E1$ event and $E1E2$ or $E1M1$ event are separated by a large energy. This condition is intuitively expected because the large separation means that the two events are independent, unrelated contributions to the scattering. Turning back to the quartz results, we find that the relations $I_p(\nu, P_2) = I_p(-\nu, -P_2)$, $p = 0, 1, 2$, holds well as shown in Table 2. It is inferred that the $E1E1$ event and $E1E2$ or $E1M1$ event are well separated and $\cos\eta \cong 0$, moreover that the parity-odd event is probably $E1E2$ but not $E1M1$ because of the energy separation. Note that the main contribution at the resonant energy at Si $1s$ is the $E1E1$ event and that the $E1E1$ event differentiates the structural chirality.

We have developed a new method to identify the absolute crystal chirality using the resonant diffraction with circularly polarized X-ray beam. Both L berlinite and L quartz show higher azimuth-constant intensity for the $(-)$ helicity beam than that for the $(+)$ helicity beam for reflection 001. The relation is opposite for R quartz. Theoretical calculation shows that this relation completely agrees with the experimental findings for the enantiomorphic space-group pair $P3_121$ and $P3_221$. This method is applicable to chiral motifs that occur in biomolecules, liquid crystals, ferroelectrics, and multiferroics, etc. We hope the present results motivate further experiments on the role of circularly polarized resonant X-ray diffraction for the study of chirality.

We thank K.S. Knight, V.E. Dmitrienko and A.M. Glazer for valuable discussions. We are grateful to D.F. Croxall who supplied the berlinite crystals. We appreciate the experimental collaboration with the soft X-ray team at RIKEN. This work was supported by Grants-in-Aid for Scientific Research (A) No. 21244049 from JSPS.

References

1. Y. Tanaka, et al., Phys. Rev. Lett. **100**, 145502 (2008)
2. Y. Tanaka, et al., Phys. Rev. Lett. **108**, 019901 (2012)
3. S.W. Lovesey, et al., J. Phys.: Condensed Matter **20**, 272201 (2008)
4. Y. Tanaka, et al., Phys. Rev. B **81**, 144104 (2010)
5. Y. Tanaka, et al., Phys. Rev. B **84**, 219905 (2011)
6. Y. Tanaka, et al., J. Phys.: Condensed Matter **22**, 122201 (2010)
7. A.M. Mulders, et al., Phys. Rev. B **81**, 092405 (2010)
8. A.M. Glazer, K. Stadnicka, J. Appl. Crystallogr. **19**, 108 (1986)
9. L.D. Landau, E.M. Lifshitz, *Quantum Electrodynamics*, vol. 4, 2nd edn. (Pergamon Press, Oxford, 1982)
10. S.W. Lovesey, S.P. Collins, *X-ray Scattering and Absorption by Magnetic Materials* (Clarendon Press, Oxford, 1996)
11. J. Als-Nielsen, D. McMorrow, *Elements of Modern X-ray Physics* (John Wiley & Sons, Ltd., New York, 2001)
12. B.E. Warren, *X-ray Diffraction* (Dover Publications, Inc., New York, 1990)
13. H. Ohashi, et al., AIP Conf. Proc. **879**, 523 (2007)
14. K. Shirasawa, et al., Phys. Rev. ST Accel. Beams **7**, 020702 (2004)
15. S.W. Lovesey, et al., Physics Reports **411**, 233 (2005)
16. N. Thong, D. Schwarzenbach, Acta Crystallogr., Sect. A: Cryst. Phys., Diffr., Theor. Gen. Crystallogr. **35**, 658 (1979)